



Pore constitution and tortuosity factor of reactively synthesized porous TiAl intermetallic compound

Yao JIANG, Yue-hui HE, Hai-yan GAO

State Key Laboratory of Powder Metallurgy, Central South University, Changsha 410083, China

Received 7 April 2020; accepted 28 September 2020

Abstract: The pore constitution and tortuosity factor of porous TiAl intermetallic were studied on the basis of the variation behavior of pore structure parameters and the discrete particle model. The pore formation mechanism of porous TiAl is mainly ascribed to three aspects: the clearance space in green compact, the diffusive pores in the reaction process and the phase transition pores, resulting in the open porosities of 5.6%, 42.9% and 1.3%, respectively. According to the Hagen–Poiseuille equation, the tortuosity factor of porous TiAl is determined in the range of 1.3–2.2. Based on the discrete particle model and the variation rule of the tortuosity factor, the tortuosity factor depends mainly on the parameters of fabrication constant, particle shape factor, clearance distance and powder particle size. The quantitative relationships among them have been established, which can be used as the basis for adjusting the pore structure of porous intermetallics.

Key words: pore constitution; tortuosity factor; TiAl intermetallics; porous material; reactive synthesis

1 Introduction

Reactive synthesis process has been a widely used method for the preparation of porous intermetallics through the Kirkendall effect [1–4]. In the process, elemental powders are used as raw materials and a relatively slow chemical reaction between them occurs by means of the solid-phase diffusion. The synthesized porous intermetallics tend to have unique pore structure characteristics [5–7], such as good coordination of multiple pore formation mechanisms, uniform pore size distribution, smooth pore walls, and relatively small tortuosity factor. Compared with porous alloys or compounds prepared through physical mechanisms, such reactively synthesized porous intermetallics generally have better material properties [8–10], including fluid permeability, structural stability and mechanical properties.

As an example of porous intermetallics, porous

TiAl alloy is a typical lightweight and high-strength material [1,11–14]. Porous TiAl intermetallic has good controllability of pore structure [15], resistance to environmental corrosion [16] and oxidation resistance at high temperature [1], showing a broad application prospect in the fields of fluid transmission such as filtration, separation, purification and throttling [1,12,17]. Currently, the parameters used to characterize the pore structure characteristics of porous TiAl mainly include the maximum aperture, open porosity, pore size distribution and permeability [1,5,15,18–20]. To some extent, these parameters reflect the macro characteristics of the pore structure. The studies on the formation mechanism of pores and the influencing factors of microscopic pore structure are of great significance for the in-depth understanding and the quantitative control of porous structure. However, the microscopic pore structure characteristics, including the tortuosity factor and pore constitution, were

rarely investigated.

In this work, porous TiAl was prepared by the reactive synthesis process of Ti and Al elemental powders. The changes of pore structure parameters in the synthesis process were analyzed, and the pore constitution caused by different pore formation mechanisms was revealed. Furthermore, the tortuosity factor of porous TiAl was calculated by combining the pore structure parameters and the Hagen–Poiseuille equation, and the quantitative relationships between the synthesis parameters and the tortuosity factor were determined.

2 Experimental

Ti and Al elemental powders with the purity of over 98.5 wt.% were used as raw materials. The average particle size ranges from 33 to 125 μm . The reactive synthesis process of porous TiAl intermetallic was carried out by a powder metallurgy method including mixing, cold pressing and vacuum sintering. The mixing procedure of elemental powders was based on the nominal composition of Ti–35wt.%Al without adding any binder or pore-making agent. The drum-type dry mixing process was adopted with the rotating speed of 40–60 r/min and the time of 6–10 h. The green compacts were formed by the single-axis mould pressing method with the pressure in the range of 80–420 MPa and the holding time of 5–10 s. In the vacuum sintering stage, the stepwise heating process [5] was adopted for the synthesis of porous TiAl intermetallic. The final sintering temperature was 1300 °C with the vacuum pressure of 10^{-2} – 10^{-3} Pa. In order to investigate the variation behavior of the increase rate of open porosity with the sintering temperature, the compacts were kept at 560, 580, 600, 620, 640, 660, 680, 700, 750, 800, 850, 900, 950, 1000, 1050, 1100, 1200 and 1300 °C for 1 h with the heating rate of 5 °C/min.

The average particle size of elemental powder was determined by laser diffraction particle size analyzer (Micro-Plus). The open porosity of porous TiAl intermetallic was measured by the Archimedes method [1]. The pore size was determined by the bubble point method [7]. The gas permeability was measured by the gas permeating method [21]. Pore constitution was determined by measuring the changes of pore structure parameters of compacts during the reactive sintering procedure. The

difference value ($\Delta\theta/\Delta T$) of open porosity (θ) with respect to sintering temperature (T) was used to characterize the rate of porosity increment with temperature. Tortuosity factor was calculated by measuring pore structure parameters and combining with the Hagen–Poiseuille equation [6,22]. The quantitative relationships between the tortuosity factor and the synthesis parameters were determined under a range of preparation conditions and related parameters, including the raw powder size and the pressing pressure.

3 Results and discussion

3.1 Pore formation

The reactive synthesis process of porous Ti–Al intermetallic compounds has been extensively studied [1,5,23–25]. In terms of the composition of Ti–35wt.%Al, which is in the composition range of γ -TiAl phase, the reaction procedure of elemental powders is mainly divided into two stages [1,26,27]: (1) the formation of TiAl₃ phase before the melting point of elemental Al, and (2) the formation of TiAl phase at the final sintering temperature. The pore size and porosity in the two stages are shown in Table 1. The porosity of reactively synthesized porous intermetallics is generally attributed to the Kirkendall effect [1]. The asymmetric diffusion behavior of the fast diffusion element generates the supersaturated vacancies, and the collapse of the vacancies leads to the continuous generation and growth of the pores. According to the change value of pore structure parameters in Table 1, the increment of the open porosity in the first stage is 1.96 times that at the second stage, while the increment of the maximum pore size in the first stage is only 0.35 times that at the second stage. This means that, at the stage of rapid diffusion of elemental Al to Ti, the evolution of the pore structure is mainly manifested in the generation of new pores, showing the characteristics of pore nucleation. After that, the evolution of pore structure mainly lies in the enlargement of relatively large pores, namely the pore growth behavior. It is worth noting that the increase in porosity in the first stage is also associated with the synthesis of TiAl₃ phase. The formation of TiAl₃ phase is a highly exothermic reaction procedure [28], which results in the melting of Al phase. The reaction process of Ti and liquid Al

Table 1 Pore structure parameters of compacts sintered at different stages compared with green compact

Stage	Maximum aperture/ μm	Open porosity/%	Reaction
Green compact	$d_0=2.3$	$\theta_0=9.8$	Ti+Al elemental powders
Compact sintered at 660 °C	$d_1=d_0+5.9$	$\theta_1=\theta_0+26.5$	$3\text{Ti}+3\text{Al}\rightarrow 2\text{Ti}+\text{TiAl}_3$
Compact sintered at 1300 °C	$d_2=d_1+16.7$	$\theta_2=\theta_1+13.5$	$2\text{Ti}+\text{TiAl}_3\rightarrow 3\text{TiAl}$

accelerates the rapid consumption of elemental Al, which promotes the formation of a large number of pores in the compact.

For the Kirkendall effect, the pore formation is correlated with the diffusion coefficient difference between the elements. The relation between the diffusion coefficient and the temperature follows the Arrhenius equation:

$$D=D_0 \exp\left(-\frac{Q}{RT}\right) \quad (1)$$

where D and T are the diffusion coefficient and the diffusion temperature, respectively; D_0 is a constant; Q and R are the diffusion activation energy and the molar gas constant, respectively.

The molar fraction of vacancies $N_v(r,t)$ at time t and position r is related to the difference of diffusion coefficients [29], which is equal to the difference of diffusion coefficients of Al and Ti elements in the Ti–Al binary system.

$$N_v(r,t)=-\int_0^t \frac{1}{r^2} \frac{\partial}{\partial r} [r^2 (D_{\text{Al}}^* - D_{\text{Ti}}^*) \frac{\partial N_{\text{Al}}}{\partial r}] dt^* \quad (2)$$

where N_{Al} is the molar fraction of Al; D_{Al}^* and D_{Ti}^* are the diffusion coefficient parameters of Al and Ti elements, respectively; t^* is the time parameter.

The maximum fraction of the Kirkendall pores in the volume can be determined if all of the vacancies condense to form voids [29].

$$\theta_v(r,t)=\frac{N_v(r,t)}{1+N_v(r,t)} \quad (3)$$

where $\theta_v(r,t)$ is the maximum Kirkendall porosity.

By combining Eqs. (2) and (3) with the Arrhenius equation, it can be concluded that the porosity generated through the Kirkendall effect is

directly related to the difference in the diffusion coefficients of elements, and is further affected by the diffusion temperature.

3.2 Pore constitution

In order to further reveal the pore structure change behavior of porous TiAl intermetallic in the reactive synthesis process, the increment rate of open porosity of Ti–Al compact at a series of sintering temperatures was measured, as shown in Fig. 1. In the reactive sintering procedure of Ti–Al system, with the increase of the sintering temperature, the diffusion coefficients of Ti and Al elements increase rapidly according to Eq. (1). Meanwhile, in the high temperature diffusion process, there is a large difference in diffusion coefficients between Ti and Al elements [30]. According to Eqs. (2) and (3), the Kirkendall porosity will continuously increase. On the other hand, the decrease in the specific surface energy of powder particles in the compact as the driving force of sintering promotes the densification process of the material at high temperature, which would lead to the decrease of the porosity. However, due to the high chemical and structural stability of TiAl intermetallic compound, its densification process in the vacuum sintering procedure is limited. This is verified by the data in Fig. 1, that is, the compact of TiAl intermetallic still maintains a positive porosity increment rate at the final sintering temperature of 1300 °C.

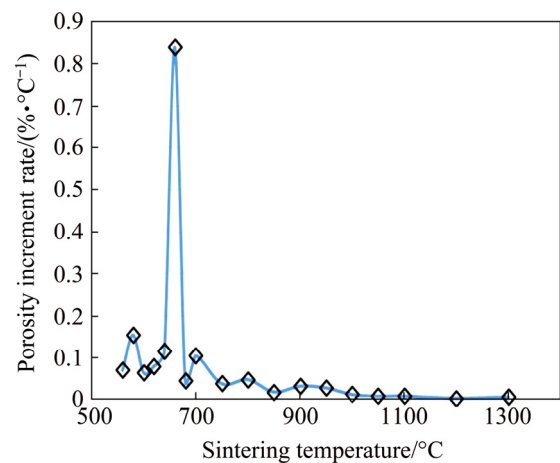


Fig. 1 Variation of increment rate of open porosity of porous Ti–35wt.%Al compact with increasing sintering temperature

From the overall trend of the variation behavior, the increment rate of porosity increases

first and then decreases with the increase of temperature, and reaches the maximum at 660 °C. The mechanism of this change includes two aspects: (1) the driving force of the increase of porosity, that is, the increasing diffusion coefficient of elements with the increase of temperature, and (2) the resistance of the porosity increment, which is mainly manifested in the continuous consumption of the reactants with high concentration gradient along with the formation of intermetallic compound phase during the reaction process. Obviously, the porosity will not increase when the composition in the compact is completely homogenized. At 660 °C, which is close to the melting point of Al metal, the large diffusion rate of Al element leads to the acceleration of pore formation rate. It was confirmed by XRD studies that TiAl₃ phase was the only intermetallic compound formed during reaction between Ti and Al at temperatures below 1000 °C [28]. The generation of TiAl₃ phase results in the large consumption of elemental Al [26], which is the main reason for the decrease in the increment rate of porosity after 660 °C.

In fact, in the process of reactive synthesis of porous intermetallic compounds, the pore formation mechanisms mainly include three aspects [31,32]: (1) the clearance space in the green compact, (2) the Kirkendall effect caused by the difference in the diffusion rates of elements, and (3) the phase transition effect caused by the density difference between resultants and reactants. When the density of the resultants is higher than that of the reactants, the phase transition pores will be formed around the particles due to the volume contraction of the particles under the condition of no mass loss. The densities of resultants and reactants at different stages in Ti–Al system are shown in Table 2. Due to the formation of TiAl₃ phase, a certain amount of pores could be generated in the compact due to the volume shrinkage of the reaction product. However, the phase transition porosity decreases to some extent due to the expansion of the product volume in the subsequent formation procedure of TiAl

phase. Considering that the effect of closed porosity is limited, the volume of the final sintered compact is used as the reference to calculate the open porosity. The open porosities originating from the interstitial pores in the green compact, the diffusive pores in the reaction process, and the phase transition pores are calculated to be 5.6%, 42.9% and 1.3%, respectively. The contributions of the clearance space, the diffusion reaction and the phase transition process to the total open porosity are about 11%, 86% and 3%, respectively.

3.3 Tortuosity factor

Tortuosity factor of porous material is defined as the ratio of the actual length of pores to the apparent one [6,35], which is an important pore structure parameter characterizing the structure of tortuous pores and the resistance of porous structure to fluid penetration. Under the condition of similar porosity and pore size, relatively small tortuosity factor is helpful to reduce the resistance of pore structure and improve the permeability. Tortuosity factor (τ) can be calculated by using the Hagen–Poiseuille equation [6,35]:

$$K = \frac{d^2 \theta}{32 \eta H \tau} \quad (4)$$

where K , d , θ and H are the permeability, pore size, open porosity and sample thickness of porous material, respectively, and η is the dynamic viscosity of fluid. The thickness of porous TiAl samples in this work is in the range of 2–3 mm. Figure 2 shows the change behavior of the tortuosity factor of porous Ti–35wt.%Al intermetallic with the particle size of raw powders. When the particle size is within the range of 33–125 μm , the tortuosity factor of porous TiAl intermetallic ranges from 1.35 to 2.09. With the increase of particle size, the tortuosity factor increases linearly, and the relation between them can be fitted as follows:

$$\tau = k_d d_g + C_d \quad (5)$$

Table 2 Density, volume shrinkage ratio and porosity due to phase transition effect at different reaction stages for Ti–35wt.%Al compound

Stage	Average density of reactant/(g·cm ⁻³)	Resultant density/(g·cm ⁻³)	Volume shrinkage ratio/%	Porosity/%
Sintered at 660 °C	$\rho_{(\text{Ti}+3\text{Al})}=3.18$	$\rho_{\text{TiAl}_3}=3.36$ [33]	3.5	1.8
Sintered at 1300 °C	$\rho_{(2\text{Ti}+\text{TiAl}_3)}=3.78$	$\rho_{\text{TiAl}}=3.76$ [34]	-1.0	-0.5

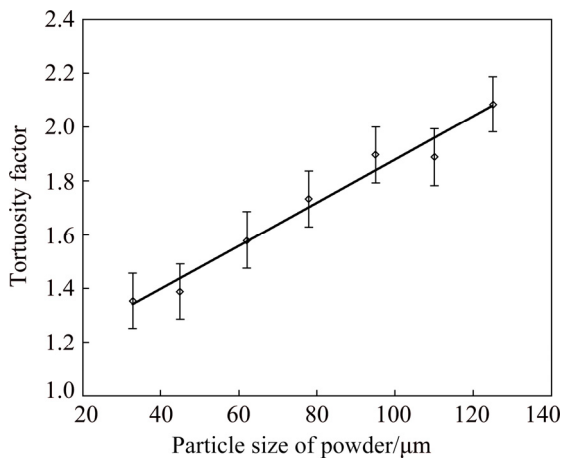


Fig. 2 Relation between tortuosity factor and particle size of powder for porous Ti–35wt.%Al intermetallic compound

where d_g is the average particle size of raw powders; k_d and C_d are the constants with the values of $8.02 \times 10^{-3} \mu\text{m}^{-1}$ and 1.08, respectively, which are obtained from the fitting results of the experimental data. The determination coefficient (R^2) for Eq. (5) is 0.97, which means a good linear fitting degree.

In order to further reveal the constitution and influence factors of tortuosity factor for porous TiAl intermetallic, a discrete particle model is used for the analysis and calculation. Figure 3 shows the positional and dimensional relationship between the pore channels and the particle skeletons in this model.

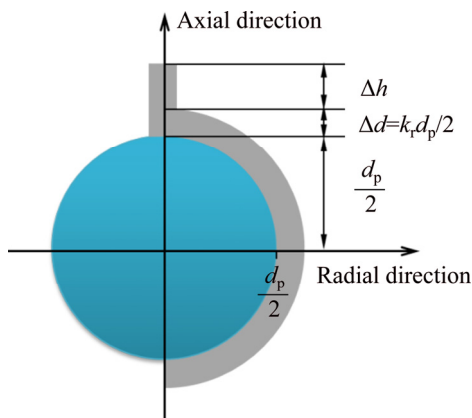


Fig. 3 Schematic diagram of tortuosity factor constitution of porous intermetallic compound in discrete particle model

According to the definition of the tortuosity factor, the following equation is obtained:

$$\tau = \frac{\frac{1}{2} \varepsilon d_p + 2\Delta d + \Delta h}{d_p + 2\Delta d + \Delta h} \tag{6}$$

where $\Delta d = k_r d_p / 2$, k_r is the fabrication constant related to the preparation conditions including the pressing pressure, sintering process, etc; ε is the particle shape factor, which is equal to π when the particle is spherical; d_p and Δh are the particle size in the compacts and the clearance distance between the particles with the size of pore channel around the particle deducted, respectively. The tortuosity factor can be expressed as follows in terms of the particle size:

$$\tau = \frac{\varepsilon/2 + k_r}{1 + k_r} \left(\frac{\varepsilon/2 - 1}{1 + k_r} \right) \frac{\Delta h}{(1 + k_r)d_p + \Delta h} \tag{7}$$

The monotonicity of the relation function of the tortuosity factor and the particle size depends on the particle shape. When $\varepsilon = 2$, that is, the particles are one-dimensional fibers, the tortuosity factor is independent of the particle size, and is a constant with the value of 1. As a typical example, when the particle shape is spherical or more complex, it means that ε is not less than π . According to Eq. (7), the tortuosity factor decreases with the decrease of the particle size. At the same time, it can be inferred that as the particle size with any shape approaches 0, the tortuosity factor approaches 1, which is basically consistent with the rule revealed by Eq. (5).

Figure 4 shows the quantitative relationship between the tortuosity factor of porous Ti–35wt.%Al intermetallic and the pressing pressure. The tortuosity factor is in the range of 1.74–2.18 when the pressing pressure ranges from 80 to 420 MPa. The tortuosity factor increases linearly with the increase of the pressing pressure of

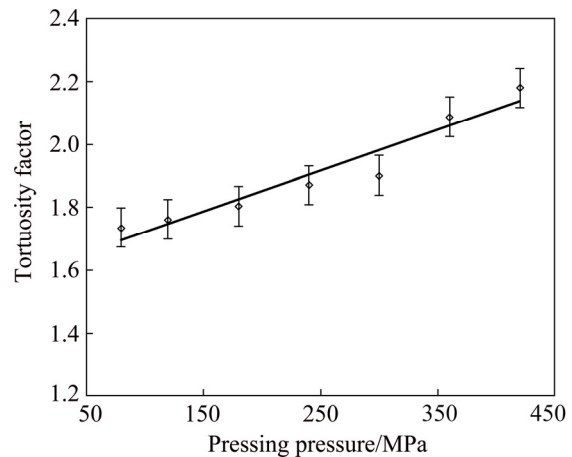


Fig. 4 Relation between tortuosity factor and pressing pressure for porous Ti–35wt.%Al intermetallic compound

the green compact, and the relationship between them can be fitted as follows:

$$\tau = k_p P + C_p \quad (8)$$

where P is the pressing pressure of the green compacts; k_p and C_p are the constants with the values of $1.29 \times 10^{-3} \text{ MPa}^{-1}$ and 1.59, respectively, which are obtained from the fitting results of the experimental data. The determination coefficient (R^2) for Eq. (8) is 0.93, which indicates an approximately linear relation between the parameters.

The change of the pressing pressure will directly affect the clearance distance ($2\Delta d + \Delta h$) between particles in the compact. The tortuosity factor in Eq. (6) can be expressed as follows in terms of the clearance distance:

$$\tau = 1 + \left(\frac{\varepsilon}{2} - 1 \right) \left(1 - \frac{1}{\frac{d_p}{2\Delta d + \Delta h} + 1} \right) \quad (9)$$

When the pressing pressure increases, the clearance distance between particles in the compact, that is, the linear section in Fig. 3, decreases accordingly. More importantly, the axial deformation of the particles increases with the increase of the pressing pressure. In particular, when the pressure increases to such an extent that the stress on the particles in the compact exceeds the yield strength, the particles will produce plastic deformation along the direction of pressure. Obviously, the plastic deformation of the particles results in an increase of the particle shape factor ε . According to Eq. (9), when the pressing pressure increases, $2\Delta d + \Delta h$ is reduced with the particle shape factor ε increasing at the same time, which will lead to the monotone increasing of the tortuosity factor. It is worth pointing out that Eq. (8) obtained by fitting the experimental data is actually a linear approximation of Eq. (9) within a certain pressure range. Furthermore, in Eq. (8), the tortuosity factor is equal to C_p (about $\pi/2$) when the pressing pressure approaches 0. In fact, when the pressing pressure is small enough, which means that the powder particles in the compact do not produce any elastic or plastic deformation, the shape factor ε can be considered to be close to π for spherical particles. At the same time, due to the fact that d_p is much larger than $2\Delta d + \Delta h$, according to

Eq. (9), the tortuosity factor of the porous material is close to $\pi/2$, which is basically consistent with the corollary result of Eq. (8).

4 Conclusions

(1) The pores of porous TiAl intermetallic are composed of the interstitial pores in the green compact, the Kirkendall pores and the pores generated by the phase transition process, and their contributions to the total open porosity are 11%, 86% and 3%, respectively.

(2) A discrete particle model for the tortuosity factor of porous TiAl intermetallic is established, in which the tortuosity factor is determined by the fabrication constant, the particle shape factor, the clearance distance and the powder particle size.

(3) The monotonicity of the relation function of the tortuosity factor and the powder particle size depends on the particle shape factor. The tortuosity factor decreases monotonously with the decrease of the particle size when the shape factor is greater than 2.

(4) There is approximately a linear relationship between the tortuosity factor and the pressing pressure. The change of the pressing pressure results in the changes in the clearance distance and the particle shape factor, which ultimately affects the tortuosity factor.

Acknowledgments

The authors are grateful for the financial supports from the National Natural Science Foundation of China (51971251, 51774336).

References

- [1] HE Y H, JIANG Y, XU N P, ZOU J, HUANG B Y, LIU C T, LIAW P K. Fabrication of Ti–Al micro/nanometer-sized porous alloys through the Kirkendall effect [J]. *Advanced Materials*, 2007, 19: 2102–2106.
- [2] LIU Xin-li, ZHANG Hui-bin, JIANG Yao, HE Yue-hui. Characterization and application of porous Ti_3SiC_2 ceramic prepared through reactive synthesis [J]. *Materials and Design*, 2015, 79: 94–98.
- [3] SHEN Bo-tao, HE Yue-hui, WANG Zhong-he, YU Lin-ping, JIANG Yao, GAO Hai-yan. Reactive synthesis of porous FeSi intermetallic compound [J]. *Journal of Alloys and Compounds*, 2020, 826: 154227.
- [4] ZHANG Hui-bin, SHEN Shu-yu, LIU Xin-li, WANG Zhong-he, JIANG Yao, HE Yue-hui. Oxidation behavior of porous Ti_3SiC_2 prepared by reactive synthesis [J].

- Transactions of Nonferrous Metals Society of China, 2018, 28: 1774–1783.
- [5] JIANG Y, HE Y H, XU N P, ZOU J, HUANG B Y, LIU C T. Effects of the Al content on pore structures of porous Ti–Al alloys [J]. *Intermetallics*, 2008, 16: 327–332.
- [6] GAO Hai-yan, HE Yue-hui, ZOU Jin, XU Nan-ping, LIU C T. Tortuosity factor for porous FeAl intermetallics fabricated by reactive synthesis [J]. *Transactions of Nonferrous Metals Society of China*, 2012, 22: 2179–2183.
- [7] WANG Zhong-he, JIANG Yao, LIU Xin-li, HE Yue-hui. Pore structure of reactively synthesized nanolaminate Ti_3SiC_2 alloyed with Al [J]. *Ceramics International*, 2020, 46: 576–583.
- [8] ZHANG Hui-bin, GAO Hai-yan, LIU Xin-li, YU Hang, WANG Long-fei, JIANG Yao, GAO Lin, YU Lin-ping, HE Yue-hui, CHEN Xiao-ming, ZHANG Lei, ZHENG Guo-qu. Reactive synthesis and assessment of porous Fe–20.5Al–18Cr intermetallic material: A comparative study with porous FeCrAl material produced from prealloyed powders [J]. *Separation and Purification Technology*, 2019, 220: 152–161.
- [9] GAO H Y, HE Y H, ZOU J, SHEN P Z, JIANG Y, LIU C T. Mechanical properties of porous Fe–Al intermetallics [J]. *Powder Metallurgy*, 2015, 58: 197–201.
- [10] LIU Xin-li, JIANG Yao, ZHANG Hui-bin, HE Yue-hui. Corrosion behavior of porous Ti_3SiC_2 in nitric acid and aqua regia [J]. *Transactions of Nonferrous Metals Society of China*, 2017, 27: 584–590.
- [11] PENG Qin, YANG Bin, LIU Li-bin, SONG Chang-jiang, FRIEDRICH B. Porous TiAl alloys fabricated by sintering of TiH_2 and Al powder mixtures [J]. *Journal of Alloys and Compounds*, 2016, 656: 530–538.
- [12] WAN Ling, WANG Zhan-Yi, WEI Xing, LI Ji-Yang, ZHONG Guang-Wei, DUAN Xiao-Peng, HE Fu-Yuan, JIANG Yao, WANG Dong-Sheng. Mechanism of anti-arterial thrombosis of Dahuangzhecong Fang screened by Ti–Al intermetallic compound porous material [J]. *Transactions of Nonferrous Metals Society of China*, 2012, 22: 3156–3160.
- [13] JIAO Xin-yang, WANG Xiao-hong, FENG Pei-zhong, LIU Ya-nan, ZHANG Lai-qi, AKHTAR F. Microstructure evolution and pore formation mechanism of porous TiAl_3 intermetallics via reactive sintering [J]. *Acta Metallurgica Sinica (English Letters)*, 2018, 31: 440–448.
- [14] LU Zhong-liang, XU Wen-liang, CAO Ji-wei, XIA Yuan-lin, DENG Qing-hua, LI Di-chen. Microstructures and properties of porous TiAl-based intermetallics prepared by freeze-casting [J]. *Transactions of Nonferrous Metals Society of China*, 2020, 30: 382–391.
- [15] CHEN M R, JIANG Y, HE Y H, LIN L W, HUANG B Y, LIU C T. Pore evolution regulation in synthesis of open pore structured Ti–Al intermetallic compounds by solid diffusion [J]. *Journal of Alloys and Compounds*, 2012, 521: 12–15.
- [16] ZHENG Zhi, JIANG Yao, DONG Hong-xing, TANG Lie-min, HE Yue-hui, HUANG Bai-yun. Environmental corrosion resistance of porous TiAl intermetallic compounds [J]. *Transactions of Nonferrous Metals Society of China*, 2009, 19: 581–585.
- [17] JIANG Yao, HE Yue-hui, LIU Xin-li, GAO Hai-yan. Application of porous TiAl intermetallic compound in purification of industrial TiCl_4 liquid in Ti metallurgy [J]. *Materials Research Express*, 2020, 7: 026511.
- [18] WANG F, LIANG Y F, SHANG S L, LIU Z K, LIN J P. Nb–Al diffusion reaction in high Nb containing TiAl porous alloys [J]. *Materials Science and Technology*, 2015, 31: 1388–1391.
- [19] JIAO Xin-yang, WANG Xiao-hong, KANG Xue-qin, FENG Pei-zhong, ZHANG Lai-qi, WANG Jian-zhong, AKHTAR F. Hierarchical porous TiAl_3 intermetallics synthesized by thermal explosion with a leachable space-holder material [J]. *Materials Letters*, 2016, 181: 261–264.
- [20] LIANG Yong-feng, YANG Fan, ZHANG Lai-qi, LIN Jun-pin, SHANG Shun-li, LIU Zi-Kui. Reaction behavior and pore formation mechanism of TiAl–Nb porous alloys prepared by elemental powder metallurgy [J]. *Intermetallics*, 2014, 44: 1–7.
- [21] ZHANG Hui-bin, LIU Xin-li, JIANG Yao, GAO Lin, YU Lin-ping, LIN Nan, HE Yue-hui, LIU C T. Direct separation of arsenic and antimony oxides by high-temperature filtration with porous FeAl intermetallic [J]. *Journal of Hazardous Materials*, 2017, 338: 364–371.
- [22] JIANG Yao, HE Yue-hui. Reactive synthesis of asymmetric porous TiAl intermetallic compound membrane [J]. *Materials Research Express*, 2019, 6: 1165g5.
- [23] AWAD A S, MERHEB D, ZAKHOUR M, NAKHL M, BOBET J L. Rapid and direct reactive synthesis of Ti–Al intermetallics by microwave heating of TiH_2 and Al powder without microwave susceptor [J]. *Journal of Alloys and Compounds*, 2017, 720: 182–186.
- [24] SINA H, IYENGAR S. Reactive synthesis and characterization of titanium aluminides produced from elemental powder mixtures [J]. *Journal of Thermal Analysis and Calorimetry*, 2015, 122: 689–698.
- [25] LIU Cheng-cheng, LU Xin, YANG Fei, TONG Jian-bo, XU Wei, WANG Zhe, QU Xuan-hui. Preparation of TiAl alloy powder by reactive synthesis in molten KCl–LiCl salt [J]. *JOM*, 2018, 70(10): 2230–2236.
- [26] JIANG Yao, HE Yue-hui. Swelling behavior of porous Ti–35%Al alloy prepared by reactive synthesis [J]. *Chinese Journal of Materials Research*, 2010, 24: 191–195. (in Chinese)
- [27] JIANG Y, HE Y H, HUANG B Y, ZOU J, HUANG H, XU N P, LIU C T. Criterion to control self-propagation high temperature synthesis for porous Ti–Al intermetallics [J]. *Powder Metallurgy*, 2011, 54: 404–407.
- [28] SUJATA M, BHARGAVA S, SANGAL S. On the formation of TiAl_3 during reaction between solid Ti and liquid Al [J]. *Journal of Materials Science Letters*, 1997, 16: 1175–1178.
- [29] MASUMURA R A, RATH B B, PANDE C S. Analysis of Cu–Ni diffusion in a spherical geometry for excess vacancy production [J]. *Acta Materialia*, 2002, 50: 4535–4544.
- [30] MISHIN Y, HERZIG C. Diffusion in the Ti–Al system [J]. *Acta Materialia*, 2000, 48: 589–623.
- [31] GAO H Y, HE Y H, SHEN P Z, JIANG Y, LIU C T. Effect of pressure on pore structure of porous FeAl intermetallics [J]. *Advanced Powder Technology*, 2015, 26: 882–886.
- [32] WANG Zhong-he, ZHANG Hui-bin, LIU Xin-li, JIANG Yao, GAO Hai-yan, HE Yue-hui. Reactive synthesis of porous nanolaminate $\text{Ti}_3(\text{Si,Al})\text{C}_2$ intermetallic compound [J].

- Materials Chemistry and Physics, 2018, 208: 85–90.
- [33] PANG J C, CUI X P, LI A B, FAN G H, GENG L, ZHENG Z Z, WANG Q W. Effect of solid solution of Si on mechanical properties of TiAl₃ based on the multi-laminated Ti–(SiC_p/Al) composite system [J]. Materials Science & Engineering A, 2013, 579: 57–63.
- [34] SCHUMACHER G, DETTENWANGER F, SCHUTZE M, HORNAUER U, RICHTER E, WIESER E, MOLLER W. Microalloying effects in the oxidation of TiAl materials [J]. Intermetallics, 1999, 7: 1113–1120.
- [35] CHAKRABARTI S. A novel experimental setup to study the Hagen-Poiseuille and Bernoulli equations for a gas and determination of the viscosity of air [J]. European Journal of Physics, 2015, 36: 065046.

反应合成多孔 TiAl 金属间化合物的孔隙组成和曲折因子

江 焱, 贺跃辉, 高海燕

中南大学 粉末冶金国家重点实验室, 长沙 410083

摘 要: 根据孔结构参数的变化规律和离散粒子模型, 研究多孔 TiAl 金属间化合物的孔隙组成和曲折因子。结果表明, 多孔 TiAl 的孔隙形成机理主要归因于 3 个方面: 生坯中的间隙空间、反应过程中的扩散孔隙和相变孔隙, 所产生的开孔隙度分别为 5.6%、42.9%和 1.3%。根据 Hagen–Poiseuille 方程, 确定多孔 TiAl 的曲折因子在 1.3~2.2 范围内。综合离散粒子模型和曲折因子的变化规律, 曲折因子主要取决于制备常数、颗粒形状、间隙距离和粉末粒度等参数。建立曲折因子与制备参数之间的定量关系, 可作为调整多孔金属间化合物孔结构的依据。

关键词: 孔隙组成; 曲折因子; TiAl 金属间化合物; 多孔材料; 反应合成

(Edited by Xiang-qun LI)